Two proteolytic pathways regulate DNA repair by cotargeting the Mgt1 alkylguanine transferase

Cheol-Sang Hwang, Anna Shemorry, and Alexander Varshavsky[1]

Division of Biology, California Institute of Technology, Pasadena, CA 91125

Contributed by Alexander Varshavsky, December 9, 2008 (sent for review November 22, 2008)

O^6-methylguanine (O^6meG) and related modifications of guanine in double-stranded DNA are functionally severe lesions that can be produced by many alkylating agents, including *N*-methyl-*N′*-nitro-*N*-nitrosoguanidine (MNNG), a potent carcinogen. O^6meG is repaired through its demethylation by the O^6-alkylguanine-DNA alkyltransferase (AGT). This protein is called Mgmt (or MGMT) in mammals and Mgt1 in the yeast *Saccharomyces cerevisiae*. AGT proteins remove methyl and other alkyl groups from an alkylated O^6 in guanine by transferring the adduct to an active-site cysteine residue. The resulting S-alkyl-Cys of AGT is not restored back to Cys, so repair proteins of this kind can act only once. We report here that *S. cerevisiae* Mgt1 is cotargeted for degradation, through a degron near its N terminus, by 2 ubiquitin-mediated proteolytic systems, the Ubr1/Rad6-dependent N-end rule pathway and the Ufd4/Ubc4-dependent ubiquitin fusion degradation (UFD) pathway. The cotargeting of Mgt1 by these pathways is synergistic, in that it increases not only the yield of polyubiquitylated Mgt1, but also the processivity of polyubiquitylation. The N-end rule and UFD pathways comediate both the constitutive and MNNG-accelerated degradation of Mgt1. Yeast cells lacking the Ubr1 and Ufd4 ubiquitin ligases were hyperresistant to MNNG but hypersensitive to the toxicity of overexpressed Mgt1. We consider ramifications of this discovery for the control of DNA repair and mechanisms of substrate targeting by the ubiquitin system.

N-end rule | proteolysis | Ubr1 | Ufd4 | yeast

Since the 1987 discovery that a key DNA repair protein, Rad6, was a ubiquitin (Ub)-conjugating enzyme (1, 2), there have been great strides in understanding the massive, multilevel involvement of the Ub–proteasome system in the DNA damage response (reviewed in refs. 3 and 4). A major aspect of this response is the repair of damage caused by alkylating agents such as *N*-methyl-*N′*-nitro-*N*-nitrosoguanidine (MNNG) and methyl methane sulfonate (MMS), which produce both mutagenic and cytotoxic lesions in DNA (4, 5). One functionally severe lesion in double-stranded DNA is O^6-methylguanine (O^6meG), which is demethylated by the O^6-alkylguanine-DNA alkyltransferase (AGT). This protein is called Mgmt (or MGMT) in mammals and Mgt1 in the yeast *Saccharomyces cerevisiae* (5–8). Compounds that produce O^6meG in DNA are common environmental carcinogens. Some of these compounds are also formed as a part of normal cellular metabolism. The repair of O^6meG in DNA is down-regulated in many cancers, usually because of lower than normal levels of Mgmt in cancer cells. Consequently, some anticancer drugs are DNA alkylating agents whose targets include O^6 in guanine. An acquired or preexisting resistance of cancer cells to such drugs often involves an up-regulation of Mgmt (4, 5). AGT proteins remove methyl and other alkyl groups from alkylated O^6 in guanine by transferring an adduct to an active-site Cys residue (5, 6). The resulting S-alkyl-Cys residue of AGT is not restored back to Cys, so repair proteins of this kind can act only once. In mammals, the alkylated (inactive) Mgmt and possibly the unmodified Mgmt are short-lived proteins, degraded by an unknown pathway (9). In human cells that express the E6 protein of the human papilloma virus (HPV), MGMT is also targeted for degradation by a complex of the viral E6 protein and E6AP, one of mammalian HECT-domain E3 Ub ligases (8, 10).

In this study, we discovered that Mgt1, the O^6meG-DNA alkyltransferase of *S. cerevisiae*, is a physiological substrate of both the Ubr1-dependent N-end rule pathway and the Ufd4-dependent Ub fusion degradation (UFD) pathway (Fig. 1). *S. cerevisiae* Mgt1 is a 188-residue protein that is sequelogous (similar in sequence) (11) to mammalian Mgmt (7, 12, 13).

The N-end rule relates the in vivo half-life of a protein to the identity of its N-terminal residue (2, 14–17). Degradation signals (degrons) that are targeted by the N-end rule pathway include a set called N-degrons (2, 15). The main determinant of an N-degron is a destabilizing N-terminal residue of a substrate protein. The N-end rule has a hierarchic structure that involves the primary, secondary, and tertiary destabilizing N-terminal residues (Fig. 1*A*). Destabilizing activities of these residues differ by their requirements for a preliminary enzymatic modification (refs. 2 and 15–18 and references therein). E3 Ub ligases of the N-end rule pathway are called N-recognins (15, 17, 19–21). They bind to primary destabilizing N-terminal residues of N-end rule substrates. The *S. cerevisiae* N-end rule pathway contains a single N-recognin, Ubr1, a 225-kDa sequelog (11) of mammalian Ubr1 and Ubr2 (Fig. 1*A*) (19–23). The functions of the N-end rule pathway (Fig. 1*A*) include the sensing of nitric oxide (NO), oxygen, heme, and short peptides; the maintenance of the high fidelity of chromosome segregation; the control of peptide import; regulation of signaling by transmembrane receptors, through the NO/O_2-dependent degradation of regulators of G protein signaling (RGS) proteins that down-regulate G proteins; specific functions of the pancreas; regulation of apoptosis, meiosis, spermatogenesis, neurogenesis, and cardiovascular development in mammals; and regulation of leaf senescence in plants (refs. 2, 17, 18, and 21–25 and references therein).

The UFD pathway was discovered through the use of engineered Ub fusions in which the structure of either the N-terminal Ub moiety or its junction with a downstream polypeptide inhibited the cleavage of a Ub fusion by deubiquitylating enzymes (DUBs) (14, 26, 27). Genetic dissection of the UFD pathway in *S. cerevisiae* identified Ufd1–Ufd5 as proteins that were required, either strictly or in part, for the degradation of engineered UFD substrates (27, 28). Ufd4 is the 168-kDa HECT-domain E3 enzyme of the UFD pathway, which functions together with the E2 enzymes Ubc4 or Ubc5. Distinct domains of Ufd4 were shown to recognize the N-terminal Ub moiety of UFD substrates (29) and also specific subunits of the 26S proteasome (30, 31). Ufd4 plays a role in the conditional autoubiquitylation and degradation of the Ubc7 E2 enzyme (32). Rad4, a nucleotide excision repair protein, is partially stabilized in *ufd4*Δ cells, suggesting that Rad4 may be a substrate of the UFD pathway (33).

Besides its relevance to DNA repair, the identification of *S. cerevisiae* Mgt1 DNA alkyltransferase as a physiological sub-

Author contributions: C.-S.H., A.S., and A.V. designed research; C.-S.H. and A.S. performed research; C.-S.H., A.S., and A.V. analyzed data; and C.-S.H., A.S., and A.V. wrote the paper.

The authors declare no conflict of interest.

[1]To whom correspondence should be addressed. E-mail: avarsh@caltech.edu.

This article contains supporting information online at www.pnas.org/cgi/content/full/0812316106/DCSupplemental.

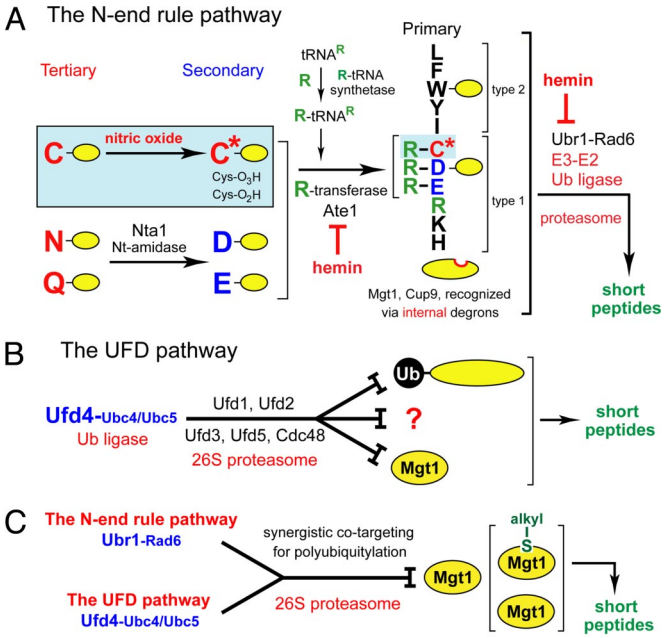

Fig. 1. The N-end rule pathway, the UFD pathway, and cotargeting of the Mgt1 DNA alkyltransferase by these proteolytic systems. (*A*) The *S. cerevisiae* N-end rule pathway. N-terminal residues are indicated by single-letter abbreviations for amino acids. Yellow ovals denote the rest of a protein substrate. Primary, secondary, and tertiary denote mechanistically distinct subsets of destabilizing N-terminal residues. Hemin (Fe^{3+}-heme) inhibits the arginylation activity of the *ATE1*-encoded Arg-tRNA-protein transferase (R-transferase), and also inhibits a subset of Ubr1 functions (24). Reactions in the shaded rectangle are a part of the pathway that is active in multicellular eukaryotes, which produce NO (18), and is also relevant to eukaryotes such as *S. cerevisiae*, which lack NO synthases but can produce NO by other routes and can also be influenced by NO from extracellular sources. C* denotes oxidized Cys, either Cys-sulfinate or Cys-sulfonate. (*B*) The *S. cerevisiae* UFD pathway. Previously known artificial (engineered) UFD substrates have in common a ''nonremovable'' N-terminal Ub moiety, which functions as a degron in the UFD pathway (14, 26, 27). Mgt1 is the first physiological UFD substrate that lacks an N-terminal Ub moiety and is not a component of the Ub system (see *Introduction*). A question mark denotes the expectation of other UFD substrates. (*C*) Cotargeting of Mgt1 by the N-end rule and UFD pathways.

strate of both the N-end rule and UFD pathways (Fig. 1) brings together 2 mechanistically distinct targeting systems, in that Ubr1 is a RING-type E3, whereas Ufd4 is a HECT-type E3. The N-end rule and UFD pathways were the first specific pathways of the Ub system to be discovered (14). Studies of these pathways have been proceeding largely in parallel (2, 14, 15, 26–29, 31, 33), until the present discovery of their functional and mechanistic connection, as described below.

Results and Discussion

N-End Rule Pathway Targets Mgt1 for Degradation. Large-scale identification of *S. cerevisiae* protein complexes through coimmunoprecipitation and other assays suggested that the 225-kDa Ubr1 E3 Ub ligase (Fig. 1*A*) may physically interact with Ygl081w, Pex7, Yak1, Mgt1, Ccr4, Gal80, and Srs2 [see supporting information (SI) *Materials and Methods* and the legend to Fig. S1]. We asked whether any of these putative Ubr1 ligands were short-lived in vivo, and, if so, whether they were degraded at least in part by the N-end rule pathway. We used a "cycloheximide-chase" assay with wild type (wt) versus *ubr1*Δ *S. cerevisiae*. In this method, the in vivo levels of a protein of interest are determined by SDS/PAGE and immunoblotting (IB) of cell extracts as a function of time after the inhibition of translation by cycloheximide. A majority of the above proteins were found to metabolically unstable. However, the absence of Ubr1 stabilized just one of these proteins, Mgt1 (Fig. S1*A*), the sole O^6-methylguanine DNA-alkyltransferase in *S. cerevisiae* (see *Introduction*).

Although the inferred ORF of *S. cerevisiae* Mgt1 contains 2 in-frame start codons, 18 codons apart (7), only the smaller, 188-residue Mgt1 is produced in vivo (13). We replaced the chromosomal *MGT1* gene with an otherwise identical ORF expressing $Mgt1_{m13}$ (C-terminally tagged with 13 copies of the 10-residue *m*yc epitope) from the endogenous P_{MGT1} promoter. $Mgt1_{m13}$ was indistinguishable from wt *MGT1* in its ability to protect cells from MNNG, a DNA-alkylating agent (Fig. S1*C*). The instability of $Mgt1_{m13}$ could be restored by reintroducing *UBR1* into *ubr1*Δ cells (Fig. 2*A*). Importantly, this rescue did not occur with $Ubr1^{C1220S}$, an inactive Ubr1 mutant (20) (Fig. 2*A*).

A cycloheximide-chase assay monitors the in vivo decay of both "young" and "old" molecules of a test protein. To assess the metabolic fate of newly formed Mgt1, we carried out pulse–chase assays with ^{f}DHFR-Ub^{K48R}-$Mgt1^{f}$ ["f" denotes the flag epitope linked to the N terminus and C terminus of the dihydrofolate reductase (DHFR) and Mgt1 moieties, respectively]. DUBs cotranslationally cleave this Ub fusion at the Ub^{K48R}-$Mgt1^{f}$ junction, yielding the long-lived reference ^{f}DHFR-Ub^{K48R} and the test protein $Mgt1^{f}$. In this Ub-reference technique (refs. 23 and 25 and references therein), the free ^{f}DHFR-Ub^{K48R} serves as a "built-in" reference protein to compensate for scatter of expression levels and immunoprecipitation efficiency, thereby increasing the accuracy of pulse–chase assays. The in vivo half-life ($t_{1/2}$) of $Mgt1^{f}$ at 30 °C was ≈19 min in wt cells and ≈32 min in *ubr1*Δ cells (Fig. S2*A*), consistent with the results of cycloheximide-chase assays (Fig. S1*A*), including the residual instability of Mgt1 in *ubr1*Δ cells.

We also used the *pdr5*Δ *S. cerevisiae* strain, in which the absence of the Pdr5 transporter allows the intracellular accumulation of MG132, a proteasome inhibitor. No $Mgt1_{m13}$-linked polyUb "ladders" were detected in wt cells in the absence of MG132 (Fig. S1*B*, lanes 1 and 2), suggesting that polyubiquitylation of Mgt1 (in contrast to its subsequent destruction by the proteasome) was rate-limiting under these conditions. Consistent with this interpretation, larger, presumably polyubiquitylated forms of $Mgt1_{m13}$ appeared after the treatment of cells for 1 h with MG132 (Fig. S1*B*, lanes 1 and 2 versus lanes 3 and 4). The levels of MG132-induced $Mgt1_{m13}$ derivatives were much lower in *ubr1*Δ cells but were still detectable (Fig. S1*B*, lane 4 versus lane 6), suggesting that another Ub ligase may also target Mgt1. In a different assay, $Mgt1_{ha}$ (C-terminally ha-tagged) was coexpressed in wt *S. cerevisiae* with His_6-tagged $Ub^{K48R,G76A}$, a double-mutant Ub that can become a part of polyUb chains but would inhibit their disassembly by DUBs (ref. 2 and references therein). *S. cerevisiae* was treated with MNNG, and polyubiquitylated proteins were isolated from cell extracts by using His_6-specific chromatography, followed by SDS/PAGE and IB with anti-ha antibody. A smear of high-M_r, $Mgt1_{ha}$-containing proteins was observed near the top of the gel, whereas such proteins were virtually absent in a test with His_6-lacking $Ub^{K48R,G76A}$ (Fig. 2*B*).

The Ub ligase holoenzyme of the N-end rule pathway is Ubr1-Rad6, in which the 20-kDa Rad6 is the Ub-conjugating enzyme (E2) (15, 20). To determine whether other E2s might also play a role, we carried out cycloheximide-chase assays with a collection of E2-null mutants that expressed $Mgt1_{f3}$ (wt Mgt1 C-terminally tagged with 3 copies of the flag epitope). $Mgt1_{f3}$ was strongly stabilized only in *rad6*Δ cells (Fig. S1*D*, lanes 5 and 6). In addition to being the E2 of the Ubr1 E3, Rad6 also functions as a part of Ub ligases that contain, in particular, the Bre1, Ubr2, or Rad18 E3s (34). In cycloheximide-chase assays with null mutants in these E3s, Mgt1 was significantly stabilized only in *ubr1*Δ cells (Fig. 2*D*). Interestingly, the degradation of Mgt1 was accelerated in a *ubr2*Δ strain, compared with its wt counterpart (Fig. 2*D*, lanes 5 and 6; compare with lanes 1 and 2). Ubr2 is a sequelog of Ubr1 that also functions in a complex with

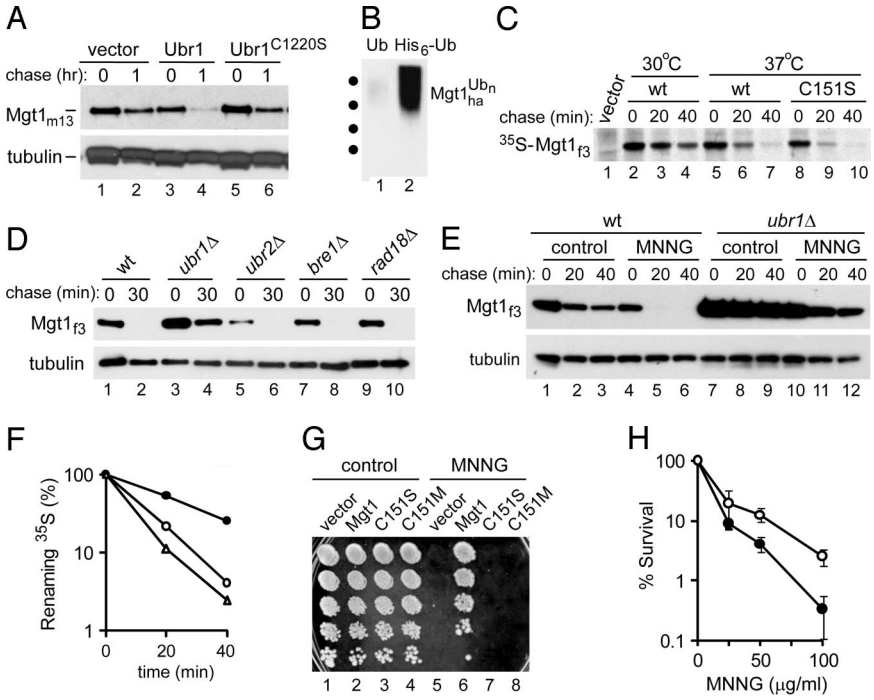

Fig. 2. Mgt1 as a physiological substrate of the N-end rule pathway. (*A*) CHY108, a *ubr1*Δ strain of *S. cerevisiae* that expressed $Mgt1_{m13}$ (Mgt1 C-terminally tagged with 13 myc epitopes) (see *SI Materials and Methods* and Table S1) was transformed with pRS315 (vector alone), with pCH100 (expressing wt Ubr1), or with pCH159 (expressing inactive $Ubr1^{C1220S}$) (20). Cultures were grown to an A_{600} of ≈1 in SD medium, followed by a ''chase'' with cycloheximide for 1 h and IB of cell extracts with either anti-myc or anti-tubulin antibodies (the latter antibody was used to verify the uniformity of total protein loads). (*B*) Polyubiquitylated $Mgt1_{ha}$, detected by IB with anti-ha antibody, in MNNG-treated cells that expressed untagged Ub (lane 1) or His_6-Ub (lane 2). Dots on the left refer to positions of molecular mass markers, at 75, 100, 150, and 250 kDa, respectively. (*C*) *S. cerevisiae* expressing $Mgt1_{f3}$ (pCH437) or $Mgt1^{C151S,f3}$ (pCH438) (Table S2) were grown in SD medium to an A_{600} of ≈0.8, then incubated further for 1 h at 30 °C or 37 °C and labeled with [^{35}S]methionine/cysteine for 5 min, followed by a chase for 0, 20, and 40 min at 30 °C or 37 °C, respectively. Cell extracts were precipitated with anti-flag antibody, followed by SDS–4–12% NuPAGE and autoradiography. (*D*) Cycloheximide ''chase'' assays with Mgt1 and *S. cerevisiae* null mutants in genes encoding the indicated E3 Ub ligases. (*E*) Wt and *ubr1*Δ *S. cerevisiae* expressing $Mgt1_{m13}$ ($Mgt1_{myc13}$) from the P_{MGT1} promoter were grown to an A_{600} of ≈0.6 and incubated further in the presence of 68 μM MNNG for 1 h, followed by a ''chase'' with cycloheximide for 20 and 40 min, SDS–4–12% NuPAGE of cell extracts, and IB with anti-myc and anti-tubulin antibodies. (*F*) Quantitation of the data in *C*, using PhosphorImager. Open and solid circles indicate $Mgt1_{f3}$ at 37 °C and at 30 °C, respectively; open triangles indicate $Mgt1^{C151S,f3}$ at 37 °C. (*G*) CHY21 (*mgt1*Δ) *S. cerevisiae* expressing $Mgt1_{f3}$ (pCH336), $Mgt1^{C151S,f3}$ (pCH337), or $Mgt1^{C151M,f3}$ (pCH338) were grown to an A_{600} of ≈0.8 at 30 °C in SD medium, followed by a further incubation for 1 h, in either the presence or absence of 68 μM MNNG. The cultures were serially diluted, spotted on YPD plates, and incubated for 3 days at 30 °C. (*H*) Colony assay for MNNG toxicity. *S. cerevisiae* YPH277 (wt) (solid circles) and YPH277HR1 (*ubr1*Δ) (open circles) were grown in YPD medium at 30 °C to an A_{600} of ≈1.0 and were further incubated for 1 h in the presence of MNNG at indicated concentrations. Cell suspensions were diluted in PBS, spread on YPD plates, and incubated for 3 days at 30 °C, followed by determination of colony numbers.

Rad6. However, in contrast to Ubr1, Ubr2 does not recognize N-degrons (35). The enhancement of Mgt1 degradation in *ubr2*Δ cells (Fig. 2*D* and Fig. S2*B*) could be caused by an increased level of Ubr1-accessible Rad6, and also, nonalternatively, by an up-regulation of the proteasome, owing to an increase in Rpn4, which is partially stabilized in *ubr2*Δ cells (35, 36).

Either MNNG or High Temperature Accelerate Mgt1 Degradation. At approximately 200 molecules per haploid cell in exponential cultures, the endogenous Mgt1 is a scarce protein in *S. cerevisiae* (12). Mgt1-dependent DNA-alkyltransferase activity in *S. cerevisiae* extracts was strongly decreased after a treatment of cells with MNNG or shifting them from 30 °C to 37 °C (12). Our results account for these effects, as the in vivo degradation of Mgt1 was accelerated by these treatments (Fig. 2*E* and Fig. S2*C*). Strong effects of increased temperature on Mgt1 degradation could be detected by either cycloheximide-chase or conventional pulse–chase assays (Fig. 2 *C* and *F* and Figs. S1*E* and S2*C*). In contrast, oxidizing agents such as H_2O_2 (Fig. S2*C*) or *t*-butyl hydroxide (data not shown) did not increase the rate of Mgt1 degradation. The acceleration of yeast Mgt1 degradation by MNNG (Fig. 2*E*) was analogous to the previously observed effects of either MNNG or O^6-benzylguanine (the latter alkylates the active-site Cys of Mgmt) on the degradation, by an unknown pathway, of Mgmt, the mammalian counterpart of Mgt1 (9). We also examined *mgt1*Δ cells that expressed either $Mgt1_{f3}$, $Mgt1^{C151M,f3}$, or $Mgt1^{C151S,f3}$. In the latter derivatives of Mgt1, the active-site Cys^{151} was replaced either by Met, a mimic of methylated Cys, or by Ser, a substitution that also inactivates Mgt1. *S. cerevisiae* expressing $Mgt1^{C151M,f3}$ or $Mgt1^{C151S,f3}$ were hypersensitive to MNNG (Fig. 2*G*). In the absence of MNNG, $Mgt1^{C151M,f3}$ was much shorter-lived than wt $Mgt1_{f3}$ (data not shown). By contrast, and in agreement with the inability of the Ser-mutant $Mgt1^{C151S,f3}$ to be alkylated at position 151, this mutant was longer-lived than wt $Mgt1_{f3}$ in cells that were treated with MNNG (Fig. 3*A*).

The 3D structure of the 22-kDa human MGMT (6), a counterpart of the 21-kDa *S. cerevisiae* Mgt1, showed that MGMT consists of a "ribonuclease-like" N-terminal domain (residues 6–92) and a C-terminal DNA-binding domain (residues 96–176) (Fig. S3 *A*, *B*, and *D*). A putative 3D structure of *S. cerevisiae* Mgt1 was modeled on human MGMT and took into account its sequelogy to Mgt1 (Fig. S4*C*). The active-site Cys of human MGMT resides between the C-terminal DNA-binding domain and the N-terminal lobe that faces away from DNA (6) (Fig. S3*B*). Our findings (see Fig. S4*A*) indicate that the degron of *S. cerevisiae* Mgt1 is close to its N terminus. Thus, the active-site Cys^{151} of Mgt1 is not a part of its degron per se. Instead, the alkylation of Cys^{151} that accompanies the repair of alkylated DNA by Mgt1 may change its conformation and/or conformational mobility and thereby increase the accessibility of its degron (which would be expected to "face away" from DNA) to cognate Ub ligases. This model is consistent with the above-mentioned faster degradation of $Mgt1^{C151M,f3}$, which contains Met^{151}, a mimic of methylated Cys, instead of wt Cys^{151}.

The absence of Ubr1 made *S. cerevisiae* ≈10-fold more resistant to MNNG, compared with wt cells (Fig. 2*H* and Fig. S2*E*). These results suggested that Ubr1 targets not only alkylated (inactive) Mgt1 but also unmodified Mgt1. This interpretation would account for the higher MNNG resistance of *ubr1*Δ cells, as the absence of degradation of unmodified Mgt1 would result in more of it available for DNA repair. In agreement with the hyperresistance of *ubr1*Δ cells to MNNG, they were also found to exhibit a lower frequency of MNNG-induced mutations (Fig. S2*D*).

Ubr1 Targets Mgt1 Via a Degron Near Its N Terminus. C-terminally truncated fragments of $Mgt1_{f3}$ were expressed in either *ubr1*Δ or wt *S. cerevisiae*, followed by SDS/PAGE of cell extracts and IB with

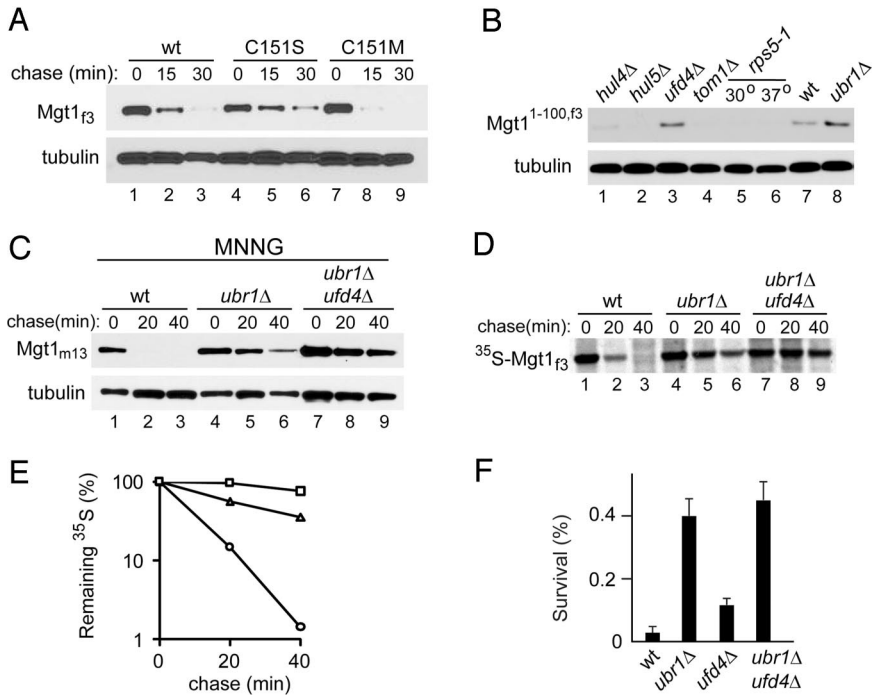

Fig. 3. The UFD pathway plays a role in degradation of Mgt1. (*A*) CHY21 (*mgt1*Δ) *S. cerevisiae* expressing $Mgt1_{f3}$ (pCH336), $Mgt1^{C151S,f3}$ (pCH337), or $Mgt1^{C151M,f3}$ (pCH338) were grown to an A_{600} of ≈0.8 at 30 °C, then incubated for 1 h with MNNG at 68 μM, followed by a "chase" with cycloheximide for 15 and 30 min, SDS–4–12% NuPAGE of cell extracts, and IB with anti-flag and anti-tubulin antibodies. (*B*) The in vivo levels of $MGT1^{1-100,f3}$ (see Fig. S4*A*) were compared by IB, using anti-flag and anti-tubulin antibodies (the latter a loading control), with extracts from wt *S. cerevisiae* and its null mutants in either Ubr1 or several HECT-type E3 Ub ligases (a *ts* mutant in the case of Rps5). $MGT1^{1-100,f3}$ was expressed in these strains from pCH372 (Table S2). Cultures were grown at 30 °C to an A_{600} of ≈0.8. Some IB assays (with *rps5-1* cells) were also carried out with extracts from cells that were incubated for 1 h at 37 °C. Note an increase of $MGT1^{1-100,f3}$ in *ufd4*Δ cells, in addition to *ubr1*Δ cells. (*C*) Wt, *ubr1*Δ, and *ubr1*Δ *ufd4*Δ *S. cerevisiae* that expressed chromosomally integrated $MGT1_{m13}$ (see *SI Materials and Methods*) were grown at 30 °C to an A_{600} of ≈0.8 and were further incubated in the presence of MNNG (68 μM) for 1 h, followed by a "chase" with cycloheximide for 20 and 40 min, SDS–4–12% NuPAGE of cell extracts, and IB with anti-myc and anti-tubulin antibodies. (*D*) Pulse–chase assays with $Mgt1_{f3}$ and wt (lanes 1–3), *ubr1*Δ (lanes 4–6), or *ubr1*Δ *ufd4*Δ (lanes 7–9) *S. cerevisiae*. Cells expressing $Mgt1_{f3}$ from the P_{MET25} promoter on a low copy plasmid were labeled for 5 min with [^{35}S]methionine/cysteine and chased for 0, 20, or 40 min, followed by immunoprecipitation with anti-flag antibody, SDS/PAGE, and autoradiography (see *SI Materials and Methods*). (*E*) Quantitation of data in *D*, using PhosphorImager. Circles, wt cells; triangles, *ubr1*Δ cells; squares, *ubr1*Δ *ufd4*Δ cells. 100% refers to the relative amount of ^{35}S at time 0 (end of pulse) for each of 3 pulse–chases. (*F*) *S. cerevisiae* of the indicated genotypes were grown to an A_{600} of ≈0.6 in YPD medium and were further incubated in either the presence or absence of MNNG (0.34 mM) for 1.5 h at 30 °C. Cell suspensions were diluted with PBS (PBS), spread on YPD plates, and incubated for 3 days at 30 °C. Survival refers to numbers of colonies in MNNG-treated samples as percentages of the corresponding numbers in untreated samples.

anti-flag antibody (Fig. S4*A*). $Mgt1^{1-100,f3}$, which contained the ribonuclease-like N-terminal domain of Mgt1 but lacked the active-site Cys^{151}, was undetectable in wt cells but readily detectable in *ubr1*Δ cells (Fig. S4*A*, lanes 5 and 6), indicating the presence of a Ubr1-specific degron in the N-terminal half of Mgt1. The results with $Mgt1^{1-144,f3}$ (Fig. S4*A*, lanes 3 and 4) were similar to those with $Mgt1^{1-100,f3}$. $Mgt1^{84-188,f3}$, an N-terminally truncated Mgt1, could not be expressed at detectable levels in either wt or *ubr1*Δ cells (Fig. S4*A*, lanes 7 and 8).

UFD and N-End Rule Pathways Cotarget Mgt1 for Degradation. Given the residual instability of Mgt1 in the absence of Ubr1 (Fig. 2 *A*, *D*, and *E*), we attempted to identify another E3 that may target Mgt1. This search involved expression of the $Mgt1^{1-100,f3}$ fragment from the P_{MGT1} promoter (Fig. S4*A*) and a set of *S. cerevisiae* mutants in several E3s (*ubr1*Δ, *ubr2*Δ, *hrd1*Δ, *hrd3*Δ, *doa10*Δ, *ufd2*Δ, *tul1*Δ, *hul4*Δ, *hul5*Δ, *ufd4*Δ, *tom1*Δ, *rps5-1*^{ts}). Among these mutants, the $Mgt1^{1-100,f3}$ fragment was significantly stabilized in *ubr1*Δ cells (as expected), and also, remarkably, in *ufd4*Δ cells (Fig. 3*B*, lane 3). Ufd4 is a 168-kDa HECT-domain E3 Ub ligase that mediates the UFD pathway (see *Introduction* and Fig. 1*B*). Given this result, we carried out cycloheximide-chase assays with wt, *ubr1*Δ, and *ubr1*Δ *ufd4*Δ double-mutant *S. cerevisiae* strains that expressed full-length $Mgt1_{m13}$. The absence of both Ubr1 and Ufd4 stabilized Mgt1 much more than the absence of Ubr1 alone (Fig. 3*C* and Fig. S2*F*). The synergistically enhanced stabilization of $Mgt1_{m13}$ in *ubr1*Δ *ufd4*Δ cells was observed either at 37 °C (Fig. S2*F*) or upon a treatment with MNNG (Fig. 3*C*). Moreover, a conventional pulse–chase assay at 37 °C with $Mgt1_{f3}$ and either wt, *ubr1*Δ, or *ubr1*Δ *ufd4*Δ cells has demonstrated a virtually complete stabilization of newly formed Mgt1 in *ubr1*Δ *ufd4*Δ cells (Fig. 3 *D* and *E*). As would be expected (given the results above), the absence of Ufd4 alone partially stabilized Mgt1, especially in *ufd4*Δ versus wt cells that were treated with MNNG (Fig. S2 *G* and *H*).

S. cerevisiae lacking Ufd4 were ≈2.5-fold more resistant to MNNG than their wt counterparts (Fig. 3*F* and Fig. S4*F*). Double-mutant *ubr1*Δ *ufd4*Δ cells, in which Mgt1 was particularly long-lived (Fig. 3 *C–E*), grew slightly slower than congenic wt cells (Fig. S4 *F* and *G* and data not shown). Moreover, overexpressing $Mgt1_{f3}$ in either wt, *ubr1*Δ, or *ufd4*Δ cells did not significantly impair their growth (data not shown) but led to a severe growth defect in *ubr1*Δ *ufd4*Δ cells (Fig. S4 *G* and *H*). Thus, the inability to destroy Mgt1 is near-lethal upon overexpression of Mgt1 and is also likely to be deleterious, to a lower extent, at physiological levels of Mgt1.

In Vitro Binding of Ubr1 and Ufd4 to Mgt1 and Cup9. The type 1 and type 2 substrate-binding sites of Ubr1 are specific for basic N-terminal residues (Arg, Lys, His) and bulky hydrophobic N-terminal residues (Trp, Phe, Tyr, Leu, Ile), respectively. The third binding site of Ubr1 recognizes an internal (non-N-degron) degradation signal of Cup9, a transcriptional repressor of a regulon that includes the Ptr2 transporter of di- and tripeptides (19, 22, 25). This binding site of Ubr1 is autoinhibited but can be allosterically activated by the binding of cognate peptides (including those imported into cells by Ptr2) to the type 1/2 sites of Ubr1. The resulting down-regulation of the Cup9 repressor, through its accelerated degradation by the N-end rule pathway, up-regulates the expression of the Ptr2 transporter. This positive-feedback circuit allows *S. cerevisiae* to detect the presence of extracellular peptides and to react by increasing their uptake (22, 23, 25). We used *cup9*Δ, *ubr1*Δ, and *cup9*Δ *ubr1*Δ mutants to determine whether the observed effect of Ubr1 on the in vivo degradation of Mgt1 (e.g., Fig. 2 *A*, *B*, *D*, and *F*) might be influenced by a circuit controlled by Cup9, and found no such influence (Fig. S4*E*).

In agreement with previous work, which used GST-pulldown assays to demonstrate the dependence of interactions between Ubr1 and GST-Cup9 on the presence of cognate (type 1/2) dipeptides (19, 22), the in vitro binding of ^{f}Ubr1 to GST-Cup9 required the presence of cognate dipeptides such as Arg-Ala (type 1 dipep-

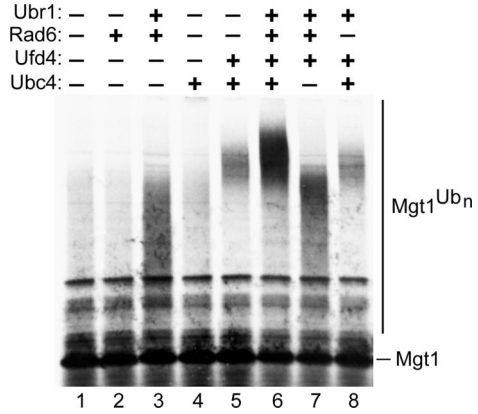

Fig. 4. Synergistic cotargeting of Mgt1 by the N-end rule and UFD pathways. The in vitro ubiquitylation system contained: Ub (80 μM), Uba1 (E1, Ub-activating enzyme, 0.1 μM), Rad6 and Ubc4 (E2, Ub-conjugating enzymes, 1 μM each), Ubr1 and Ufd4 (E3 Ub ligases, 0.2 μM each) were purified proteins. 2 μl of ^{35}S-labeled Mgt1, produced by using the TNT T7 Quick for PCR DNA and 4 mM ATP (see *SI Materials and Methods*), were added to the above reaction mixture (final volume 20 μl) or its variations, as indicated in the image, followed by incubation at 30 °C for 15 min. One half of each sample was fractionated by SDS–4–12% NuPAGE, followed by autoradiography. ^{35}S-Mgt1 and its polyubiquitylated derivatives are indicated on the right. Lane 1, S^{35}-Mgt1 (input). Lane 2, same as lane 1 but with Rad6. Lane 3, same as lane 1 but with Ubr1 and Rad6. Lane 4, same as lane 1 but with Ubc4. Lane 5, same as lane 1 but with Ufd4 and Ubc4. Lane 6, same as lane 1 but with Ubr1, Rad6, Ufd4, and Ubc4. Lane 7, same as lane 6 but without Ubc4. Lane 8, same as lane 6 but without Rad6. Note a strikingly synergistic enhancement of Mgt1 polyubiquitylation, including an increase in the mean size of Mgt1-conjugated polyUb chains in the presence of both Ubr1/Rad6 and Ufd4/Ubc4 (lane 6).

tide) and Leu-Ala (type 2 dipeptide) (Fig. S4*B*, lane 11; compare with lane 12). Analogous GST pulldowns were used to detect a specific interaction between ^{f}Ubr1 and GST-Mgt1 (Fig. S4*B*, lanes 3–9). Interestingly, this interaction did not require the presence of cognate dipeptides. Moreover, it was inhibited by the same (cognate) dipeptides at concentrations that activated the interaction of ^{f}Ubr1 with GST-Cup9 (Fig. S4*B*, lane 8, compare with lanes 3 and 9). The comparably robust but opposite effect of cognate peptides on the Ubr1-Mgt1 interaction remains to be understood in physiological terms.

As would be expected from the Ufd4-dependent degradation of Mgt1 in vivo (Fig. 3 *B–E* and Fig. S2 *G* and *H*), a GST-Mgt1 pulldown with ^{ha}Ufd4 (instead of ^{f}Ubr1) confirmed the binding of Ufd4 to Mgt1 (Fig. S4*C*). In contrast to Mgt1-Ubr1 interactions, which were inhibited by cognate type 1/2 dipeptides (Fig. S4*B*), the binding of ^{ha}Ufd4 to GST-Mgt1 occurred irrespective of type 1/2 or other tested dipeptides (Fig. S4*C*). The same results were obtained with Mgt1-GST, in which the GST moiety was C-terminal rather than N-terminal (data not shown). The Ufd4-Mgt1interaction could also be detected by using a coimmunoprecipitation assay (Fig. S4*D*).

Synergistic Enhancement of the Extent and Processivity of Mgt1 Polyubiquitylation by Ubr1 and Ufd4. We developed an in vitro system that consisted of the following purified components: Ub; Uba1 (Ub-activating enzyme, E1); Rad6 and/or Ubc4 (E2 enzymes specific for Ubr1 and Ufd4, respectively); Ubr1 and/or Ufd4 (E3s that target Mgt1); and ATP. This system also contained ^{35}S-labeled Mgt1$_{f3}$, which was produced in reticulocyte lysate (see *SI Materials and Methods*). In the final reaction mix, 10% of the total volume was contributed by the ^{35}S-Mgt1-containing reticulocyte lysate. Either the Ubr1-Rad6 Ub ligase alone or the Ufd4-Ubc4 Ub ligase alone polyubiquitylated Mgt1 in vitro (Fig. 4, lanes 3 and 5; compare with lane 1). Whereas the yield of polyubiquitylated Mgt1 was higher with Ubr1-Rad6 alone than with Ufd4-Ubc4 alone, the latter Ub ligase was more processive. Specifically, Mgt1 that was polyubiquitylated by Ufd4-Ubc4 alone migrated as a set of derivatives in a relatively narrow size range, ≈180 kDa. This molecular mass implied the presence of a polyUb chain linked to the 21-kDa Mgt1 and containing ≈19 Ub moieties (Fig. 4, lane 5). In contrast, the polyubiquitylated Mgt1 produced by Ubr1-Rad6 alone migrated as a more diffuse set of derivatives, and at a significantly lower size range, up to ≈150 kDa (Fig. 4, lanes 3 and 5; compare with lane 1).

Strikingly, the polyubiquitylation of Mgt1 in the presence of Ubr1-Rad6 and Ufd4-Ubc4 together exhibited both a higher overall yield and higher processivity. Specifically, Mgt1 that was polyubiquitylated in the presence of both the N-end rule's and UFD's Ub ligases migrated as a set of higher-yield derivatives in a relatively narrow size range, ≈200 kDa on average (Fig. 4, lane 6; compare with lanes 3 and 5). This size was higher than the one with Mgt1 with Ufd4-Ubc4 alone (Fig. 4, lane 5) and much higher than the one with Mgt1 with Ubr1-Rad6 alone (Fig. 4, lane 3; compare with lane 1). This reproducible result (Fig. 4, lane 6, and data not shown) indicated that the targeting mechanisms of the N-end rule and UFD pathways are not simply "additive" in regard to Mgt1. Specifically, this cotargeting of Mgt1, reconstituted in the in vitro system, is synergistic both in regard to yields of polyubiquitylated Mgt1 and in regard to the processivity of polyubiquitylation (Fig. 4, lanes 1, 3, 5, and 6). Operationally, the Ufd4-Ubc4 Ub ligase appears to function, in part, as an enhancer of the processivity of Mgt1 polyubiquitylation by Ubr1-Rad6 (Fig. 4). Such a role of Ufd4-Ubc4 may be analogous to the function of Ufd2, a component of the UFD pathway that Jentsch and colleagues showed to act by increasing the processivity of polyubiquitylation of UFD substrates that contain the N-terminal Ub moiety (28).

Concluding Remarks. The discovery that Mgt1, the DNA alkyltransferase of *S. cerevisiae*, is a physiological substrate of both the N-end rule pathway and the UFD pathway (Fig. 1*C*) has ramifications for the control of DNA repair not only in fungi but in other eukaryotes as well. The AGT proteins (see *Introduction*), including yeast Mgt1 and mammalian Mgmt (MGMT), are highly sequelogous (Fig. S3*D*). In addition, the N-end rule and UFD pathways are present in all eukaryotes examined (2, 14, 26–29, 33). Using a split-Ub assay, we found that mouse Ubr1 and Ubr2, 2 sequelogous N-recognins of the mammalian N-end rule pathway, interact with mouse Mgmt in vivo (J. Sheng, C.-S. H., and A. V., unpublished data), strongly suggesting that (at least) the N-end rule pathway mediates the degradation of mammalian Mgmt. Mouse *Ubr2*$^{-/-}$ fibroblasts, which lack Ubr2 and therefore contain a partially impaired N-end rule pathway, were found to be hypersensitive to mitomycin C, a DNA cross-linking agent (37). Melanoma cells that overexpress Mgmt are also hypersensitive to mitomycin C (38). Taken together with our results (Fig. 1*C*), these findings suggest that the degradation of mammalian Mgmt, presumably by both the N-end rule and UFD pathways, plays a role in determining the sensitivity of mammalian cells to alkylating agents, including some DNA cross-linking agents as well. The striking effect of simultaneous presence of the Ubr1-Rad6 and Ufd4-Ubc4 Ub ligases on both the yield and processivity of Mgt1 polyubiquitylation makes the in vitro system described in Fig. 4 a promising tool for further analyses of Mgt1 targeting. It should be possible to make this assay better defined through the provision of purified Mgt1, currently the system's sole unpurified component (Fig. 4). Questions that can be addressed by this approach include specific location(s) and topology of Mgt1-linked polyUb chains that are produced by the Ubr1-Rad6 versus Ufd4-Ubc4 Ub ligases.

The in vivo destruction of Mgt1 that had become alkylated (through the repair of alkylated DNA by Mgt1) may occur at or near the sites of repaired DNA lesions. A priori, it is likely (nothing is known about this at present) that Mgt1 functions as a part of chromosome-associated protein complexes. If so, the subunit se-

lectivity of the N-end rule pathway, i.e., its ability to remodel a protein complex by destroying a subset of its subunits while sparing the rest of them (39), might play a role in the in vivo degradation of Mgt1. This process may be analogous to the previously discovered selective degradation, by the N-end rule pathway, of the separase-produced fragment of Scc1, a subunit of chromosome-associated cohesin complexes (40). This degradation of the Scc1 fragment is essential for the high fidelity of chromosome segregation (40). Both the alkylated (inactive) Mgt1 protein (Fig. 1*C*) and the separase-produced fragment of the Scc1 cohesin subunit (40) are obligatory in vivo products of the corresponding circuits. These proteins are also "dead-end" structures. Under conditions where the Scc1 fragment cannot be eliminated by the N-end rule pathway, this protein can be shown to perturb chromosome mechanics (40). A chromosome-bound, alkylated but unremoved Mgt1 may present an analogous problem. Thus, the N-end rule and UFD pathways operate, in these contexts, as homeostasis-maintaining devices that employ their capacity for subunit-selective protein remodeling (39) to reset the states of relevant circuits. Because *ubr1*Δ, *ufd4*Δ, and particularly *ubr1*Δ *ufd4*Δ cells were hyperresistant (rather than hypersensitive) to the toxicity of MNNG (Fig. 3*F*), a precise role of the N-end rule and UFD pathways vis-a-vis DNA repair and other cellular functions remains to be understood. For example, a homeostatic role of these pathways in removing, through degradation, the alkylated (chromosome-bound?) Mgt1 may be important not for the repair of alkylated DNA per se but for another chromosome-associated process(es) that would be either halted or function suboptimally in the presence of unremoved Mgt1. This interpretation is consistent with a strong toxicity of overexpressed Mgt1 in *ubr1*Δ *ufd4*Δ cells but not in wt cells (Fig. S4 *G* and *H*).

The discovery that Mgt1 is cotargeted by 2 otherwise dissimilar Ub-dependent pathways (Fig. 1) opens up new questions. For example: Might the cotargeting of Mgt1 by Ubr1 and Ufd4 (Fig. 1*C*) signify a physical interaction between these E3s? Our preliminary data suggest that Ubr1 and Ufd4 indeed interact, possibly in a conditional manner (unpublished data). Furthermore, previous work indicated that the both the Ubr1 and Ufd4 E3s interact with specific subunits of the 26S proteasome (30, 31). Thus, the demonstrated cotargeting of Mgt1 by the N-end rule and UFD pathways (Fig. 1*C*) may involve not only copolyubiquitylation of Mgt1 (Fig. 4) but proteasome-docking steps as well.

Methods

For descriptions of materials and methods, including *S. cerevisiae* strains, plasmids, and PCR primers, see *SI Materials and Methods* and Tables S1–S3. Standard techniques, including PCR, were used to construct specific plasmids and yeast strains. Specific protein components of the polyubiquitylation assay (Fig. 4) were expressed in *S. cerevisiae* or *Escherichia coli* and purified by affinity chromatography. The epitope-tagged derivatives of Mgt1, Ubr1 and Ufd4 were constructed using standard methods (see *SI Materials and Methods*), and were used in immunoblotting, coimmunoprecipitation, cycloheximide-chase, pulse–chase, GST pulldown, and either in vivo or in vitro polyubiquitylation assays with Mgt1 and its derivatives. These procedures and techniques, including specific assays for toxicity and mutagenicity of MNNG, are described, in detail, in *SI Materials and Methods*.

ACKNOWLEDGMENTS. We thank M. Longtine (Oklahoma State University, Stillwater, OK) for pFA6a-KanMX6 and pFA6a-13MYC-TRP1, Y. Xie (Wayne State University, Detroit, MI) for a collection of Ub ligase mutants, J. Li and J. Shan (Weill Cornell Medical College, New York, NY) for their assistance with Mgt1 modeling, and the present and former members of the Varshavsky laboratory, particularly J. Sheng, for their advice and assistance. This work was supported by from the National Institutes of Health Grants GM31530 and DK39520 (to A.V.), the Sandler Program for Asthma Research, and the Ellison Medical Foundation.

1. Jentsch S, McGrath JP, Varshavsky A (1987) The yeast DNA repair gene RAD6 encodes a ubiquitin-conjugating enzyme. *Nature* 329:131–134.
2. Varshavsky A (2008) Discovery of cellular regulation by protein degradation. *J Biol Chem* 283:34469–34489.
3. Harper JW, Elledge SJ (2007) The DNA damage response: Ten years after. *Mol Cell* 28:739–745.
4. Friedberg EC, *et al.* (2006) *DNA Repair and Mutagenesis* (ASM Press, Washington, DC).
5. Sedgwick B, Bates PA, Paik J, Jacobs SC, Lindahl T (2007) Repair of alkylated DNA: Recent advances. *DNA Repair* 6:429–442.
6. Wibley JEA, Pegg AE, Moody PCE (2000) Crystal structure of the human O6-alkylguanine-DNA alkyltransferase. *Nucl Acids Res* 28:393–401.
7. Xiao W, Samson L (1992) The *Saccharomyces cerevisiae* MGT1 DNA repair methyltransferase gene: Its promoter and entire coding sequence, regulation and in vivo biological functions. *Nucl Acids Res* 20:3599–3606.
8. Srivenugopal KS, Ali-Osman F (2002) The DNA repair protein, O^6-methylguanine-DNA methyltransferase is a proteolytic target for the E6 human papillomavirus oncoprotein. *Oncogene* 21:5940–5945.
9. Srivenugopal KS, Yuan X-H, Friedman SH, Ali-Osman F (1996) Ubiquitination-dependent proteolysis of O^6-methylguanine-DNA methyltransferase in human and murine tumor cells following inactivation with O^6-benzylguanine or 1,3-bis(2-chloroethyl)-1-nitrosourea. *Biochemistry* 35:1328–1334.
10. Scheffner M, Staub O (2007) HECT E3s and human disease. *BMC Biochemistry* 8 (Suppl. I):S6.
11. Varshavsky A (2004) Spalog and sequelog: Neutral terms for spatial and sequence similarity. *Curr Biol* 14:R181–R183.
12. Sassanfar M, Samson L (1990) Identification and preliminary characterization of an O^6-methylguanine DNA repair methyltransferase in the yeast Saccharomyces cerevisiae. *J Biol Chem* 265:20–25.
13. Joo JH, *et al.* (1995) Expression of yeast O^6-methylguanine-DNA methyltransferase (MGMT) gene. *Cell Mol Biol* 41:545–553.
14. Bachmair A, Finley D, Varshavsky A (1986) In vivo half-life of a protein is a function of its amino-terminal residue. *Science* 234:179–186.
15. Varshavsky A (1996) The N-end rule: Functions, mysteries, uses. *Proc Natl Acad Sci USA* 93:12142–12149.
16. Mogk A, Schmidt R, Bukau B (2007) The N-end rule pathway of regulated proteolysis: Prokaryotic and eukaryotic strategies. *Trends Cell Biol* 17:165–172.
17. Tasaki T, Kwon YT (2007) The mammalian N-end rule pathway: New insights into its components and physiological roles. *Trends Biochem Sci* 32:520–528.
18. Hu R-G, *et al.* (2005) The N-end rule pathway as a nitric oxide sensor controlling the levels of multiple regulators. *Nature* 437:981–986.
19. Xia Z, Webster A, Du F, Piatkov K, Ghislain M, Varshavsky A (2008) Substrate-binding sites of UBR1, the ubiquitin ligase of the N-end rule pathway. *J Biol Chem* 283:24011–24028.
20. Xie Y, Varshavsky A (1999) The E2–E3 interaction in the N-end rule pathway: The RING-H2 finger of E3 is required for the synthesis of multiubiquitin chain. *EMBO J* 18:6832–6844.
21. Hwang C-S, Varshavsky A (2008) Regulation of peptide import through phosphorylation of Ubr1, the ubiquitin ligase of the N-end rule pathway. *Proc Natl Acad Sci USA* 105:19188–19193.
22. Du F, Navarro-Garcia F, Xia Z, Tasaki T, Varshavsky A (2002) Pairs of dipeptides synergistically activate the binding of substrate by ubiquitin ligase through dissociation of its autoinhibitory domain. *Proc Natl Acad Sci USA* 99:14110–14115.
23. Xia Z, Turner GC, Hwang C-S, Byrd C, Varshavsky A (2008) Amino acids induce peptide uptake via accelerated degradation of CUP9, the transcriptional repressor of the PTR2 peptide transporter. *J Biol Chem* 283:28958–28968.
24. Hu R-G, Wang H, Xia Z, Varshavsky A (2008) The N-end rule pathway is a sensor of heme. *Proc Natl Acad Sci USA* 105:76–81.
25. Turner GC, Du F, Varshavsky A (2000) Peptides accelerate their uptake by activating a ubiquitin-dependent proteolytic pathway. *Nature* 405:579–583.
26. Johnson ES, Bartel BW, Varshavsky A (1992) Ubiquitin as a degradation signal. *EMBO J* 11:497–505.
27. Johnson ES, Ma PC, Ota IM, Varshavsky A (1995) A proteolytic pathway that recognizes ubiquitin as a degradation signal. *J Biol Chem* 270:17442–17456.
28. Koegl M, *et al.* (1999) A novel ubiquitination factor, E4, is involved in multiubiquitin chain assembly. *Cell* 96:635–644.
29. Ju D, Wang X, Xu H, Xie Y (2007) The armadillo repeats of the Ufd4 ubiquitin ligase recognize ubiquitin-fusion proteins. *FEBS Lett* 581:265–270.
30. Xie Y, Varshavsky A (2000) Physical association of ubiquitin ligases and the 26S proteasome. *Proc Natl Acad Sci USA* 97:2497–2502.
31. Xie Y, Varshavsky A (2002) UFD4 lacking the proteasome-binding region catalyses ubiquitination but is impaired in proteolysis. *Nat Cell Biol* 4:1003–1007.
32. Ravid T, Hochstrasser M (2007) Autoregulation of an E2 enzyme by ubiquitin-chain assembly on its catalytic residue. *Nat Cell Biol* 9:422–427.
33. Ju D, Xie Y (2006) A synthetic defect in protein degradation caused by loss of Ufd4 and Rad23. *Biochem Biophys Res Commun* 341:648–652.
34. Ullrich HD (2005) The RAD6 pathway: Control of DNA damage bypass and mutagenesis by ubiquitin and SUMO. *ChemBioChem* 6:1735–1743.
35. Wang L, Mao X, Ju D, Xie Y (2004) Rpn4 is a physiological substrate of the Ubr2 ubiquitin ligase. *J Biol Chem* 279:55218–55223.
36. Xie Y, Varshavsky A (2001) RPN4 is a ligand, substrate, and transcriptional regulator of the 26S proteasome: A negative feedback circuit. *Proc Natl Acad Sci USA* 98:3056–3061.
37. Ouyang Y, *et al.* (2006) Loss of Ubr2, an E3 ubiquitin ligase, leads to chromosome fragility and impaired homologous recombinational repair. *Mut Res* 596:64–75.
38. Passagne I, *et al.* (2006) O^6-methylguanine DNA-methyltransferase (MGMT) overexpression in melanoma cells induces resistance to nitrosoureas and temozolomide but sensitizes to mitomycin C. *Toxicol Appl Pharmacol* 211:97–105.
39. Johnson ES, Gonda DK, Varshavsky A (1990) Cis-trans recognition and subunit-specific degradation of short-lived proteins. *Nature* 346:287–291.
40. Rao H, Uhlmann F, Nasmyth K, Varshavsky A (2001) Degradation of a cohesin subunit by the N-end rule pathway is essential for chromosome stability. *Nature* 410:955–960.